

RESPONSE OF A HIGH-SPEED WAVE-PIERCING CATAMARAN TO AN ACTIVE RIDE CONTROL SYSTEM

(DOI No: 10.3940/rina.ijme.2016.a4.382)

J AlaviMehr, M R Davis, J Lavroff, D S Holloway, University of Tasmania, and **G A Thomas**, University College London

SUMMARY

Ride control systems on high-speed vessels are an important design features for improving passenger comfort and reducing motion sickness and dynamic structural loads. To investigate the performance of ride control systems a 2.5m catamaran model based on the 112m INCAT catamaran was tested with an active centre bow mounted T-Foil and two active stern mounted trim tabs. The model was set-up for towing tank tests in calm water to measure the motions response to ride control step inputs. Heave and pitch response were measured when the model was excited by deflections of the T-Foil and the stern tab separately. Appropriate combinations of the control surface deflections were then determined to produce pure heave and pure pitch response. This forms the basis for setting the gains of the ride control system to implement different control algorithms in terms of the heave and pitch motions in encountered waves. A two degree of freedom rigid body analysis was undertaken to theoretically evaluate the experimental results and showed close agreement with the tank test responses. This work gives an insight into the motions control response and forms the basis for future investigations of optimal control algorithms.

NOMENCLATURE

A_{WP}	Model equilibrium waterplane area (m^2)
d_{CF}	Distance of centre of pressure of the control surface forward of the model <i>LCF</i> (m)
d_{CG}	Distance of centre of pressure of the control surface forward of the model <i>LCG</i> (m)
d_{FG}	Distance of the model <i>LCF</i> forward of the <i>LCG</i> (m)
f_{ST}	Stern tabs lift factor (N/radian)
f_{TF}	T-Foil lift factor (N/radian)
g	Gravitational acceleration (m/s^2)
I_{CF}	Second moment of area of waterplane about a transverse axis passing through the centre of flotation (m^4)
L	Control surface lift force (N)
<i>LCF</i>	Longitudinal Centre of Flotation (m)
<i>LCG</i>	Longitudinal Centre of Gravity (m)
S	Control surface planform area (m^2)
U	Model forward speed (m/s)
x_{ST}	Distance between centre of pressure of the stern tabs and <i>LCG</i> (m)
x_{TF}	Distance between centre of pressure of the T-Foil and <i>LCG</i> (m)
α_{ST}	Stern tabs deflection (radian)
α_{TF}	T-Foil deflection (radian)
η_3	Model heave (sinkage) (m)
η_5	Model pitch (trim) (radian)
η_6	Model yaw (radian)
ρ	Water density (kg/m^3)
ω	Motion frequency ($2\pi f$)

1. INTRODUCTION

Worldwide demand for fast sea transportation has led to an on-going development of large high-speed and lightweight marine vessels for both commercial and military applications [1]. Different types of high-speed

craft have been developed to satisfy this requirement, but catamarans have proven to be most popular due to their large deck area, high hydrostatic and hydrodynamic stability and relatively large deadweight to displacement ratios [2]. INCAT Tasmania [3] has developed a unique configuration of high-speed wave-piercing catamarans with a centre bow located on the vessel centreline between the wave-piercer demihulls to effectively eliminate deck diving in following seas.

High-speed catamarans often experience large motions and accelerations. These are significantly different to those of conventional monohulls due to their high operating Froude number, slender hull shape and twin hull geometry. Catamarans experience smaller but more rapid rolling motions due to their high metacentric height, compared to large and relatively slow rolling motions of monohulls [4]. Increases in the operating speed of catamarans generally exacerbates vessel motions due to increase of Froude number which leads to passenger discomfort, sea sickness and potential structural damage when operating in severe conditions and higher sea states [5].

To increase passenger comfort and the range of operability, and reduce vessel motions and dynamic structural loads, INCAT Tasmania has used active motion control systems for its high-speed wave piercing catamarans [5, 6]. These active Ride Control Systems (RCS) consist of two active trim tabs located at the stern of the vessel demi-hulls and a retractable T-Foil mounted on the centreplane at the aft end of the centre bow. Figure 1 shows the location of the T-Foil and the stern tabs on an 112 m INCAT Tasmania high-speed wave-piercing catamaran [3]. The T-Foil generates a vertical force, either upward or downward, to reduce heave and pitch motions. Being retractable, removing the T-Foil from operation helps to reduce resistance in calm water. The trim tabs installed on the stern,

hereafter called stern tabs, produce a lift force at the transom to keep the vessel at its desired dynamic trim and also resist pitch and heave motion in combination with the T-Foil. The stern tabs can also control the roll motion of the vessel when they are deflected differentially.

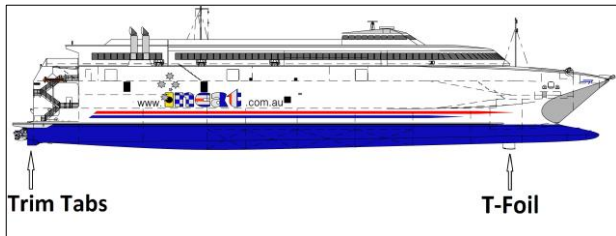


Figure 1: Location of the T-Foil and the stern tabs on an 112 m INCAT Tasmania high-speed wave-piercing catamaran (from [7]).

Although some studies on ship motions and motion control systems of INCAT Tasmania vessels have been undertaken by numerical computations and full-scale sea trials [4, 5, 7-11], there is still limited knowledge on the mechanisms of the whole motion control system. In order to understand and optimise the motion control system further investigation is required to accurately determine the effect of the control system on the ship motions and loads.

The present study investigates the step responses of the 112 m INCAT Tasmania wave-piercing catamaran to the ride control system by towing tank testing of a 2.5 m model. These calm water open-loop test results are intended to assist in the future studies of closed-loop active control system and the relative control gains with different control algorithms. The overall objective is to evaluate the effect of the ride control system on motions and loads under more controlled conditions than is possible at full scale. The motions and loads data at model scale, in conjunction with full scale sea trials data and numerical computations will ultimately assist in the optimisation of motion control system algorithms to improve ship motions, passenger comfort and reduce structural loads.

A specific purpose of the tests was to find an appropriate combination of control movements to excite the model only in heave or only in pitch. This can then form the basis of setting the gains of the ride control system to implement different control algorithms, such as pitch damping, local damping and heave damping. In addition to the experimental investigation, a numerical two Degree of Freedom (DOF) rigid-body simulation was developed to theoretically evaluate the experimental results. It should be noted that in this study the terms “sinkage” and “trim” are used rather than “heave” and “pitch” in presenting the step responses of the model to the RCS.

2. MODEL SET-UP AND INSTRUMENTATION

An existing 1/44.8 scale 2.5 m catamaran model of the 112 m INCAT Tasmania catamaran was used for the tank tests. Its development has been described previously [1, 12]. It was designed to correctly replicate the first two longitudinal bending modes of vibration and their associated frequencies, in particular for measuring wave induced dynamic slam loads and hull bending moments.

A model scale T-foil and two model scale stern tabs were designed, manufactured and fitted onto the model. Figures 2 and 3 show the electrically activated model scale stern tabs and T-foil respectively. Three stepper-motors were used independently to activate the T-Foil and stern tabs, with three potentiometers to measure their angular positions. Figures 4 and 5 show the T-Foil and its electrical actuator installed on the aft section of the centre bow. Figure 6 shows the stern tabs installed at the stern of the model.



Figure 2: Electrically activated model scale stern tabs.



Figure 3: Electrically activated model scale T-Foil.

The model scale T-Foil has previously been tested for static and dynamic lift and drag performance and frequency response using a closed-circuit water tunnel [7]. It was concluded that the model scale T-foil performs adequately for application to simulate a ride control system at full scale [7]. Similarly the tabs were tested by Bell *et al.* [8].

Experimental testing of the model was conducted with a displacement of 28.3 kg at the Australian Maritime College (AMC) towing tank in Launceston, Tasmania, simulating a full scale displacement of 2545 tonnes. The towing tank is 100 m long, 3 m wide and 1.4 m deep. The model was attached to the moving carriage using two tow posts mounted forward and aft of the model's longitudinal centre of gravity (LCG). Figure 7 shows the model attached to the moving carriage. Testing was undertaken in calm water with a primary focus on measuring the responses to the ride control system at a model speed of 2.89 m/s, simulating the full scale speed of 37 knots, while the control surfaces were deflected to various angles with rapid step movements.



Figure 4: T-Foil installed on the aft section of the centre bow.

The stepper-motors and the potentiometers were calibrated to determine the relationship between demand voltage for the stepper-motor and relative deflection of the control surface, and the relationship between the output voltage from the potentiometer and relative deflection of the control surface. During calibration the deflections of the control surfaces were measured using a digital inclinometer with a resolution of 0.05°. The inclinometer was aligned with the T-Foil chord line and the stern tabs, with 0° corresponding to these being parallel to the water surface.

Although the RCS DAQ system was able to log all the required data, a separate towing carriage data acquisition and signal conditioning system was used simultaneously to cross check the data acquired by the RCS DAQ system. LVDTs were mounted on each tow post and measured their vertical movement in order to calculate model sinkage (heave) and trim (pitch). Two video cameras were set up to record all the runs from bow and stern views.

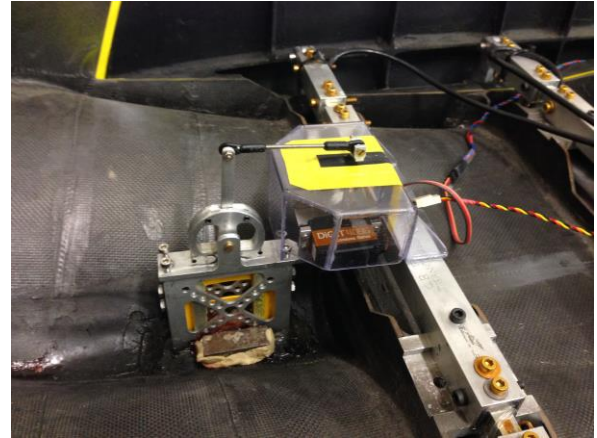


Figure 5: T-Foil electrical actuator installed on the aft section of the centre bow.



Figure 6: Stern tabs installed at the stern.

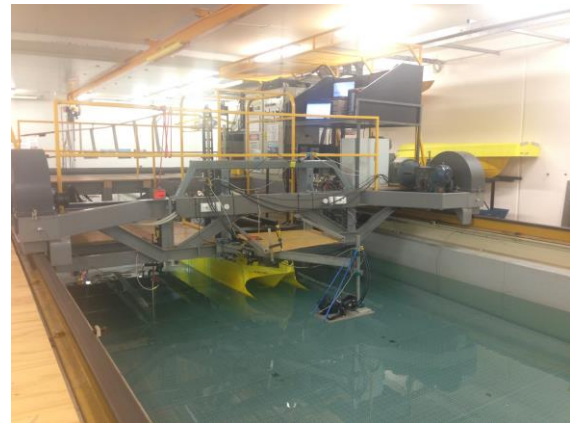


Figure 7: The catamaran model attached to the moving carriage.

3. THEORETICAL PREDICTION OF MODEL STEP RESPONSES

3.1 HYDROSTATIC PREDICTION OF STEADY STATE STEP RESPONSE

Two hydrostatic methods were used to predict the steady state response to the control surface deflections prior to conducting the model tests.

The first method, termed astatic load experiment, simulated the lift of each control surface by applying a 1.5 kg mass at the longitudinal location of each

control surface individually while the model was stationary in calm water. The sinkage and trim stiffness of the model were calculated by measuring the model movements. Figure 8 shows a schematic diagram of the model demonstrating the sign convention. Positive control deflections produce upward forces on the hull.

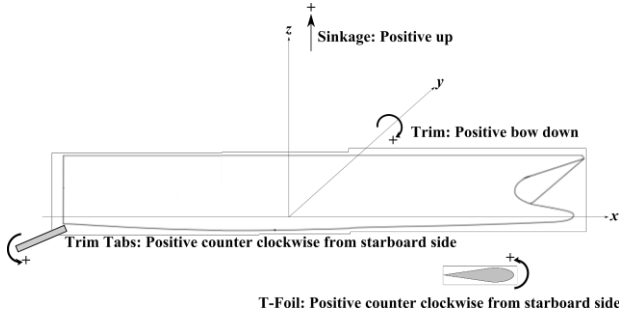


Figure 8: Schematic diagram showing the sign convention for sinkage (heave), trim (pitch), T-Foil deflection and stern tabs deflection.

Table 1 shows the results when the 1.5 kg mass was applied at the longitudinal location of T-Foil and both model movements at the longitudinal location of T-Foil and stern tabs were measured.

Table 1: Sinkage and trim stiffness calculation by applying a 1.5 kg mass at the location of T-Foil

Mass (kg)	1.5
Mass location (m, positive forward of LCG)	1.06
Observed vertical movement at the location of T-Foil (m, positive up)	-0.0135
Observed vertical movement at the location of stern tabs (m, positive up)	0.0060
Sinkage (m, positive up, measured at the LCG)	-0.0031
Trim (degree, positive bow down)	0.5614
Sinkage Stiffness (N/m)	4724.92
Trim stiffness (Nm/degree)	27.77

Table 2 shows the results when the 1.5 kg mass was applied at the longitudinal location of stern tabs and model movement at the longitudinal location of T-Foil stern tabs were measured.

Table 2: Sinkage and trim stiffness calculation by applying a 1.5 kg mass at the location of stern tabs

Mass (kg)	1.5
Mass location (m, positive forward of LCG)	-0.93
Observed vertical movement at the location of T-Foil (m, positive up)	0.0060
Observed vertical movement at the location of stern tabs (m, positive up)	-0.0110
Sinkage (m, positive up, measured at the LCG)	-0.0031
Trim (degree, positive bow down)	-0.4894
Sinkage Stiffness (N/m)	4814.29
Trim stiffness (Nm/degree)	27.95

The second method was a hydrostatic prediction which estimates the model responses using the waterplane area properties, distances between the LCF, LCG and control surface, and the lift force at each control surface.

The sinkage and trim are thus

$$\eta_3 = \frac{L}{\rho g A_{WP}} + \eta_5 d_{FG}$$

$$= \frac{L}{\rho g A_{WP}} \left(1 - \frac{A_{WP} d_{CF} d_{FG}}{I_{CF}} \right) \quad (1)$$

$$\eta_5 = \frac{-L d_{CF}}{\rho g I_{CF}} \quad (2)$$

For both methods the T-Foil lifts were then predicted using results of AlaviMehri et al. [7], while the stern tabs lifts were predicted using results of Bell et al. [8]. These were expressed in terms of a lift-curve coefficient ($\frac{dC_L}{d\alpha}$) and control surface angular deflection (α), where $\frac{dC_L}{d\alpha}$ was found to be 2.45 radian for the T-foil, 1.72 per radian for the tabs with positive deflection, and 0.40 per radian for the tabs with negative deflection.

Table 3 shows the prediction of the model response to T-Foil and stern tab deflections using the sinkage and trim stiffness determined through experimental measurement (tables 1 and 2) and the predicted sinkage and trim (equations 1 and 2) based on the empirically determined lift coefficients [7, 8]. This table shows good agreement between the two methods for predicting the steady state response to the control surface deflections.

Table 3: Prediction of model responses to the different T-foil and stern tabs deflections by using two methods of static load experiment and hydrostatic prediction

T-foil deflection (degrees)	Stern tabs deflection (degrees)	Sinkage (mm)		Trim (degrees)	
		Static load experiment	Hydrostatic prediction	Static load experiment	Hydrostatic prediction
+15	0	3.11	3.10	-0.56	-0.53
+10	0	2.07	2.06	-0.37	-0.36
-10	0	-2.07	-2.06	0.37	0.36
-15	0	-3.11	-3.10	0.56	0.53
0	+18	3.43	3.52	0.55	0.57
0	+10	1.90	1.96	0.30	0.31
0	-10	-0.51	-0.52	-0.08	-0.08
0	-18	-0.91	-0.94	-0.15	-0.15

3.2 DYNAMIC PREDICTION OF STEP RESPONSE OF MOVING MODEL USING STRIP THEORY

A numerical simulation of the experimental step responses of the model to the control surfaces deflections was developed. The general equations of motion for a six degree of freedom (DOF) rigid-body are [13]:

$$\sum_{j=1}^6 [(M_{jk} + A_{jk})\ddot{\eta}_k + B_{jk}\dot{\eta}_k + C_{jk}\eta_k] = \sum F_j \quad (j=1, \dots, 6) \quad (3)$$

where M_{jk} , A_{jk} , B_{jk} , and C_{jk} are the components of the total mass, added mass, damping, and stiffness respectively. The subscripts in $A_{jk}\ddot{\eta}_k$ refer to the force (moment) component in j -direction due to motion in the k -direction [13],

$$\begin{aligned} \eta_1 &= \text{Surge} & \eta_2 &= \text{Sway} & \eta_3 &= \text{Heave} \\ \eta_4 &= \text{Roll} & \eta_5 &= \text{Pitch} & \eta_6 &= \text{Yaw} \end{aligned}$$

It is generally accepted that in most conditions the heave and pitch equations are uncoupled from or only weakly coupled to the other degrees of freedom. In any case the experimental setup only allowed two degrees of freedom, therefore a two DOF rigid-body model was considered, as presented in Equations 4 and 5.

$$[(M + A_{33})\ddot{\eta}_3 + B_{33}\dot{\eta}_3 + C_{33}\eta_3] + [(M_{35} + A_{35})\ddot{\eta}_5 + B_{35}\dot{\eta}_5 + C_{35}\eta_5] = \sum F_3 \quad (4)$$

$$[(M_{53} + A_{53})\ddot{\eta}_3 + B_{53}\dot{\eta}_3 + C_{53}\eta_3] + [(I_{55} + A_{55})\ddot{\eta}_5 + B_{55}\dot{\eta}_5 + C_{55}\eta_5] = \sum F_5 \quad (5)$$

where, for an origin at the *LCG*

$$M_{35} = M_{53} = 0$$

$$C_{33} = \rho g A_{WP}$$

$$C_{55} = \rho g (I_{cf} + A_{WP} d_{FG}^2)$$

$$C_{35} = C_{53} = -\rho g A_{WP} d_{FG}$$

$$\sum F_3 = (\alpha_{ST} \times f_{ST}) + (\alpha_{TF} \times f_{TF}) + (-\eta_5 \times f_{TF})$$

$$\sum F_5 = (\alpha_{ST} \times f_{ST} \times x_{ST}) + (-\alpha_{TF} \times f_{TF} \times x_{TF}) + (\eta_5 \times f_{TF} \times x_{TF})$$

The f_{ST} and f_{TF} are the stern tabs and T-Foil lift factors respectively, calculated as $\frac{1}{2} \rho U^2 S \frac{dC_L}{d\alpha}$.

The added mass and damping coefficients were calculated using the following equations presented by Holloway [14], based on the theory of Salvesen et al. [15], with a T-Foil lift damping coefficient based on the equations presented by Faltinsen [13]:

$$A_{33} = \int a_{33} dx - \frac{U}{\omega^2} b_{33}^A$$

$$B_{33} = \int b_{33} dx + U a_{33}^A + \frac{1}{2} \rho U S \frac{dC_L}{d\alpha}$$

$$A_{35} = - \int (a_{33} x + \frac{b_{33} U}{\omega^2}) dx - \frac{U}{\omega^2} (a_{33}^A U - b_{33}^A x^A)$$

$$B_{35} = - \int (b_{33} x - a_{33} U) dx - U (a_{33}^A x^A + \frac{b_{33}^A U}{\omega^2}) - \frac{1}{2} \rho U S \frac{dC_L}{d\alpha} x_{TF}$$

$$A_{53} = - \int \left(a_{33}x - \frac{b_{33}U}{\omega^2} \right) dx + \frac{U}{\omega^2} b_{33}^A x^A$$

$$B_{53} = - \int \left(b_{33}x + a_{33}U \right) dx - U a_{33}^A x^A - \frac{1}{2} \rho US \frac{dC_L}{d\alpha} x_{TF}$$

$$A_{55} = \int a_{33} \left(x^2 + \frac{U^2}{\omega^2} \right) dx + \frac{U x^A}{\omega^2} (a_{33}^A U - b_{33}^A x^A)$$

$$B_{55} = \int b_{33} \left(x^2 + \frac{U^2}{\omega^2} \right) dx + U x^A (a_{33}^A x^A + \frac{b_{33}^A U}{\omega^2}) + \frac{1}{2} \rho US \frac{dC_L}{d\alpha} x_{TF}^2$$

where the superscript ^A refers to the aft or stern section. It should be pointed out that all integrals are from the bow to the stern. The two DOF rigid-body model was segmented into 40 sections at the water plane and the sectional coefficients a_{33} and b_{33} were calculated on the basis of the added mass and damping for a floating semi-circular cylinder presented by Holloway [14] shown in Figure 9 where R is the cylinder radius. Holloway has used a steady periodic Green function panel method and compared this method to an analytical solution described by Ursell in terms an infinite number of equations in an infinite number of unknowns [14]. For the purposes of calculating the sectional coefficients a_{33} and b_{33} , and global coefficients A_{ij} and B_{ij} , which are all frequency dependent, ω was taken to be the experimentally observed natural frequency.

Equations 4 and 5 can be written in matrix form as

$$\begin{bmatrix} M + A_{33} & A_{35} \\ A_{53} & I_{55} + A_{55} \end{bmatrix} \begin{bmatrix} \ddot{\eta}_3 \\ \ddot{\eta}_5 \end{bmatrix} + \begin{bmatrix} B_{33} & B_{35} \\ B_{53} & B_{55} \end{bmatrix} \begin{bmatrix} \dot{\eta}_3 \\ \dot{\eta}_5 \end{bmatrix} + \begin{bmatrix} C_{33} & C_{35} + f_{TF} \\ C_{53} & C_{55} - f_{TF} \times x_{TF} \end{bmatrix} \begin{bmatrix} \eta_3 \\ \eta_5 \end{bmatrix} = \begin{bmatrix} \alpha_{ST} \times f_{ST} + \alpha_{TF} \times f_{TF} \\ \alpha_{ST} \times f_{ST} \times x_{ST} - \alpha_{TF} \times f_{TF} \times x_{TF} \end{bmatrix} \quad (6)$$

Equation 6 is a function of T-Foil and stern tab deflection. Therefore theoretical sinkage and trim response to the control surfaces deflection, either individually or combined, can be obtained by solving Equation 6.

4. RESULTS

The model testing was carried out in calm water to investigate the step responses of the model to the ride control system. The control surfaces were first deflected individually to different angles to measure the effect of each control surface on sinkage and trim. Deflections of $\pm 15^\circ$ and $\pm 10^\circ$ were applied to the T-Foil and $\pm 18^\circ$ and $\pm 10^\circ$ to the stern tabs. Figure 8 shows a schematic diagram of the model demonstrating the sign convention.

Figures 10 to 13 compare the theoretical and experimental responses to step movements of the control surfaces when activated individually at a model test speed of 2.89 m/s.

As can be seen from Figure 10, the maximum deflection range of the T-Foil from $+15^\circ$ to -15° produces a sinkage range of about 7 mm (i.e. from +3.5 to -3.5 mm) and trim range of about 1° (i.e. ranging over $\pm 0.5^\circ$).

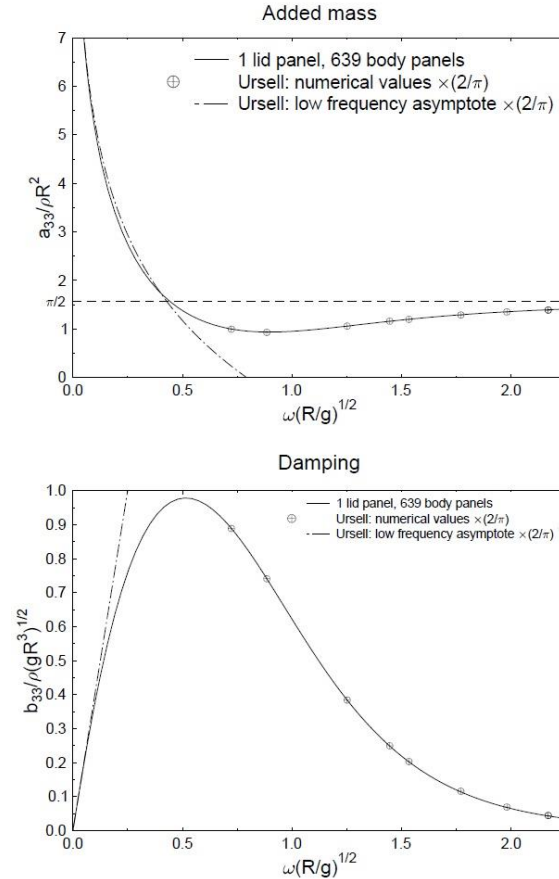


Figure 9: Heave added mass and damping for floating semi-circular cylinder (from Holloway [14])

Although the theoretical calculation of sinkage is in good agreement with experimental sinkage, the theoretical calculation over predicted the trim response by about 0.1° when the T-Foil was deflected $+15^\circ$. A possible explanation for this might be that the lift-curve coefficient ($\frac{dC_L}{d\alpha}$) was considered constant with control deflection in order to perform the theoretical prediction. However lift was not found exactly proportional to control surface deflection in previous experiments [7]. This may explain the differences of trim responses seen by the comparison of the predicted and measured trim in Figure 10 and Figure 11. The comparison between these two figures shows that experimental sinkage responses are generally consistent with the theoretical calculations of sinkage. However the deviation between theoretical sinkage and experimental sinkage is somewhat more evident in Figure 11.

Figure 12 shows that the maximum deflection of the stern tabs from -18° to $+18^\circ$ can only lift the model by about 3.5 mm but can trim the model by about 1° . As shown in Figures 12 and 13, the agreement between theoretical predictions and experimental responses to the stern tabs deflection is not as good as the results of predicted responses to T-Foil deflections presented in Figures 10 and 11. There is a small theoretical over prediction of the sinkage for positive deflections of the stern tabs, which seems to be consistent for different tab deflections as shown in Figures 12 and 13. These figures also show that the theoretical calculations somewhat under predicted the trim responses. The theoretical under prediction of trim is more significant for -10° deflection of stern tabs. A possible explanation for the stern tab results may be that the variation of the lift coefficient derivative ($\frac{dC_L}{d\alpha}$) of the stern tabs. It should be noted that two lift-coefficient derivatives ($\frac{dC_L}{d\alpha}$) were considered for positive and negative deflections of stern tabs respectively and treated as constant in each case. This was because lift was reduced for negative (i.e. upward) stern tab deflections due to flow separation from the tab. The stern tab lift-coefficient derivatives ($\frac{dC_L}{d\alpha}$) were calculated according to the results of Bell et al. [8], and these had to be extrapolated to larger angles and higher velocities. Bell et al. [8] measured the coefficients at up to only 2.31 m/s, while the tests shown in figures 12 – 15 were at 2.89 m/s. Bell et al. [8] also only measured the stern tab negative lift at an angle of attack of -7° , while up to -18° was used in the present tests. Thus some inaccuracy is expected from these extrapolations.

In these results it should be noted that a drift of the signal was observed for sinkage under the action of stern tabs only (Figure 12, sinkage), which can be explained by carriage aerodynamic effects as reported by Yang [16]. Measurements undertaken by Yang in the same towing tank as used in the present experiments demonstrated that there was flow of air between the top of the carriage and the water surface that caused a pressure wave in the vicinity of and travelling with the test model, and a corresponding (but not constant) reduction in the local calm water surface height. The experimental results presented in this study are corrected using Yang's results. In order to perform the correction for each run, a run in the same condition was performed without the control surface deflection. The repeated run without control surface deflection was considered a zero and the actual experimental step responses results were determined by subtracting the measured zero to correct for the pressure wave generated by the moving carriage. The observed drift can still be seen in some of the presented results such as in Figure 13 (left) for $t > 8$ s. This is due to the complexity of matching the time records of two different runs consisting of the non-deflected (zero) and deflected control surface model responses. This has a more significant effect when the number of repeated runs is less due to the limited data available for more

accurate correction. It should be noted that the step responses of the model to the T-Foil deflection was investigated by a higher number of runs. This produced a more accurate set of results as shown in Figures 10 and 11 as opposed to Figures 12 and 13 where the number of runs was more restricted.

Another purpose of the open loop step responses tests was to find an appropriate combination of control movements to excite the model only in sinkage or only in trim. This is needed for setting the gains of the ride control system to implement different control algorithms, such as pitch damping, local damping and heave damping. From the characteristics of the control surface actions, as discussed previously, a T-Foil deflection of $+15^\circ$ combined with a stern tab deflections of $+10^\circ$ should excite the model only in sinkage. This case is called "pure sinkage excitation". Figure 14 shows the model responses to the step movements of control surfaces when deflected together to produce "pure sinkage excitation". As can be seen this combination at model speed of 2.89 m/s can change the sinkage of the model by about 4.5 mm and the trim of the model is not changed significantly. This successful outcome confirms the control system gains required to run the ride control system in a heave damping mode. These results also show good agreement between theory and experiment.

From the previously measured control effects a T-Foil deflection of -8° together with a stern tab deflection of $+18^\circ$ should provide "pure trim excitation", and the responses are shown in Figure 15. As can be seen this combination at a model speed of 2.89 m/s changes the trim of the model by about 0.9° and the sinkage of the model is not changed. This successful outcome confirms the control system gains required to run the ride control system in a pitch damping mode. These final results shown in Figures 14 and 15 demonstrate that the theoretical calculations predicted the experimental results adequately. As can be seen in Figure 10 to 13 the most deviation between theory and experiments was observed in the second steps.

5. CONCLUSIONS

A 2.5m towing tank model of an INCAT Tasmania 112 m catamaran was equipped with a Ride Control System based on a centre bow mounted T-foil and trim tabs located at the stern of the model. Towing tank tests were performed in calm water to measure the response according to ride control step inputs to identify control gains for heave and pitch damping but also to compare the response to a numerical simulation based on a two degree of freedom rigid body analysis using strip theory.

The model experiments show that a maximum deflection of the T-Foil from $+15^\circ$ to -15° when it is operated separately can sink the model over a range of about 7mm and trim it by about 1° . Moreover a maximum deflection of the stern tabs from -18° to $+18^\circ$ lifts the model by about 3.5 mm and trims the model by about 1° .

Two hydrostatic methods were applied to predict the T-foil and stern tab responses based on a static load experiment and a hydrostatic prediction and there was close agreement between the two outcomes. This was extended by a dynamic prediction of the step response of the moving model based on a two degree of freedom rigid body analysis using strip theory. The results from this analysis developed an equation of motion to predict the sinkage and trim response of the model based on T-foil and stern tab control surface deflections. The theoretical calculation of sinkage response to the T-Foil deflection was found to be in good agreement with experimental sinkage, but over predicted the trim response by about 0.1° when the T-Foil was deflected $+15^\circ$. This is possibly due to the fact that the T-Foil lift-curve coefficient ($\frac{dC_L}{d\alpha}$) was considered constant in order to perform the theoretical analysis.

The deviation between theoretical calculations and experimental responses to the stern tabs deflection is somewhat greater than the results of predicted responses to T-Foil deflections mainly due to the lack of sufficient data to predict the lift-curve derivative of stern tabs for both positive and negative deflections at angles of $\pm 10^\circ$ and a speed of 2.89 m/s.

It was found that a T-Foil deflection of $+15^\circ$ and stern tab deflection of $+10^\circ$ produce pure sinkage, while a T-Foil deflection of -8° together with the stern tabs deflection of $+18^\circ$ leads to pure trim. These outcomes indicate the control system gains required to run the ride control system in pure pitch and pure heave damping control modes.

This study presents a reliable and relatively simple method of predicting open loop control surface step responses based on a simple strip theory, lumped parameter approach. This method and the test data obtained here can now form the basis for the optimisation of closed loop control ride control systems. The results also demonstrate that the ride control system can be operated in different damping control modes including pitch damping and heave damping when appropriate closed loop system gains are selected in the appropriate combinations for the T-foil and stern tabs. These are important outcomes and the present work now forms the basis of a comprehensive model test program to determine the control system gains required to minimise ship motions and associated loads. The development of an improved ride control system at model scale can then be used as a basis for improving the ride comfort and design of future full scale high-speed wave-piercing catamaran vessels.

6. REFERENCES

1. LAVROFF, J. DAVIS, M. R. HOLLOWAY, D. S. and THOMAS, G. "Determination of Wave Slamming Loads on High-Speed Catamarans by Hydroelastic Segmented Model Experiments,"

- International Journal of Maritime Engineering*, vol. 153, pp. A185-A197, Jul-Sep 2011.
2. THOMAS, G. WINKLER, S. DAVIS, M. HOLLOWAY, D. MATSUBARA, S. and LAVROFF, J. *et al.*, "Slam events of high-speed catamarans in irregular waves," *Journal of Marine Science and Technology*, vol. 16, pp. 8-21, Mar 2011.
3. <http://www.incat.com.au/#>. (2014).
4. DAVIS M. R. and HOLLOWAY, D. S. "Motion and passenger discomfort on high speed catamarans in oblique seas," *International shipbuilding progress*, vol. 50, pp. 333-370, 2003.
5. JACOBI, G. THOMAS, G. DAVIS, M. HOLLOWAY, D. DAVIDSON, G. and ROBERTS, T. "Full-scale motions of a large high-speed catamaran: The influence of wave environment, speed and ride control system," *International Journal of Maritime Engineering*, vol. 154, pp. A143-A155, 2012.
6. JACOBI, G. THOMAS, G. DAVIS, M. R. and DAVIDSON, G. "An insight into the slamming behaviour of large high-speed catamarans through full-scale measurements," *Journal of Marine Science and Technology*, vol. 19, pp. 15-32, Mar 2014.
7. ALAVIMEHR, J. DAVIS, M. R. and LAVROFF, J. "Low Reynolds Number Performance of a Model Scale T-Foil," *Royal Institution of Naval Architects. Transactions. Part A3. International Journal of Maritime Engineering*, vol. 157, pp. A175-A187, 2015.
8. BELL, J. ARNOLD, T. LAVROFF, J. and DAVIS, M. "Measured Loading Response of Model Motion Control Stern Tabs," *Royal Institution of Naval Architects. Transactions. Part A. International Journal of Maritime Engineering*, vol. 155, pp. A1-A7, 2013.
9. DAVIS, M. WATSON, N. and HOLLOWAY, D. "Measurement of response amplitude operators for an 86 m high-speed catamaran," *Journal of ship research*, vol. 49, pp. 121-143, 2005.
10. HOLLOWAY D. and DAVIS, M. "Ship motion computations using a high Froude number time domain strip theory," *Journal of ship research*, vol. 50, pp. 15-30, 2006.
11. SHORE, T. "Frequency Response of Motion Controls on INCAT Catamaran Model," Honors Thesis Honors Thesis, University of Tasmania, 2011.
12. LAVROFF, J. DAVIS, M. R. HOLLOWAY, D. S. and THOMAS, G. "The Vibratory Response of High-Speed Catamarans to Slamming Investigated by Hydroelastic Segmented Model Experiments," *International Journal of Maritime Engineering*, vol. 151, pp. 1-11, Oct-Dec 2009.

13. FALTINSEN, O. M. *Hydrodynamics of High-Speed Marine Vehicles*: Cambridge University Press, 2005.
14. HOLLOWAY, D. S. "A High Froude Number Time Domain Strip Theory Applied to the Sea-keeping of Semi-SWATHs," PhD, University of Tasmania, 1998.
15. SALVESEN, N. TUCK, E. O. and FALTINSEN, O "Ship motions and sea loads," *Transactions of Society of Naval Architects and Marine Engineers*, vol. 78, pp. 250-287, 1970.
16. YANG, F. "Experimental investigation on wave propagation in Australian Maritime College (AMC) towing tank and the performance of resistance and acoustic wave probes in static and moving condition," NCMEH, University of Tasmania, Australian Maritime College, 2015.

7. ACKNOWLEDGEMENTS

This project is supported by Australian Research Council *Linkage* grant No. LP-0883540. The support of INCAT Tasmania Pty. Ltd., Revolution Design Pty. Ltd., the University of Tasmania, and the Australian Maritime College is gratefully acknowledged.

APPENDICES - Figures: 10-15

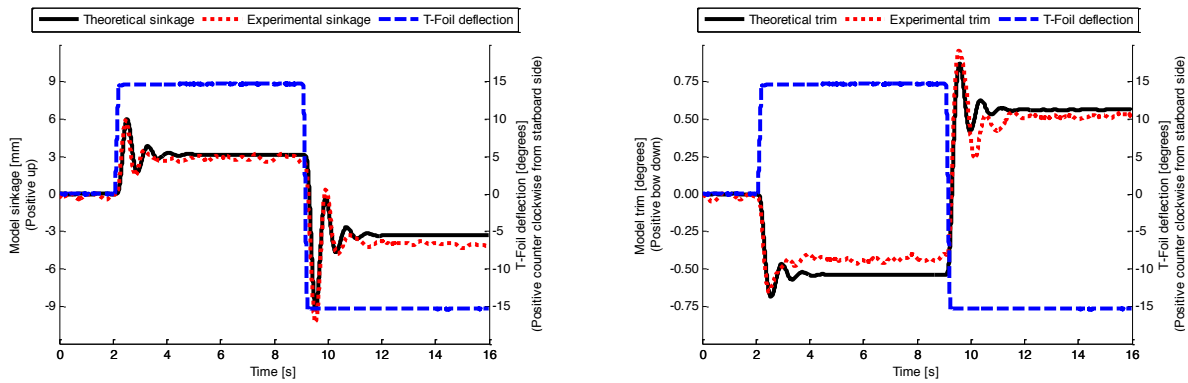


Figure 10: Model responses to T-Foil deflection of $\pm 15^\circ$ at model speed of 2.89m/s

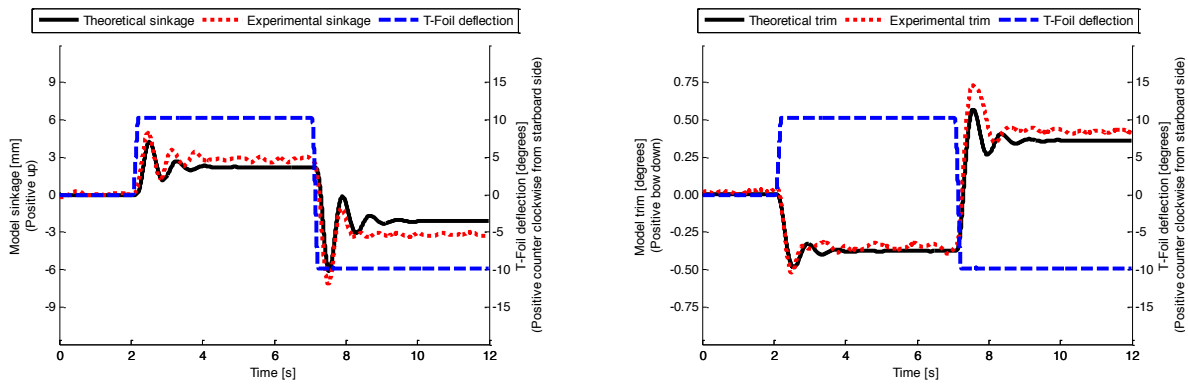


Figure 11: Model responses to T-Foil deflection of $\pm 10^\circ$ at model speed of 2.89m/s

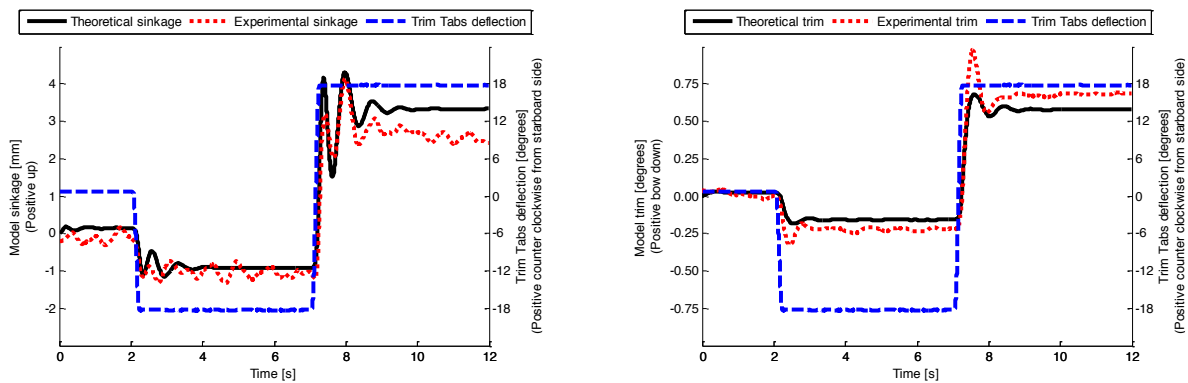


Figure 12: Model responses to stern tabs deflection of $\pm 18^\circ$ at model speed of 2.89m/s

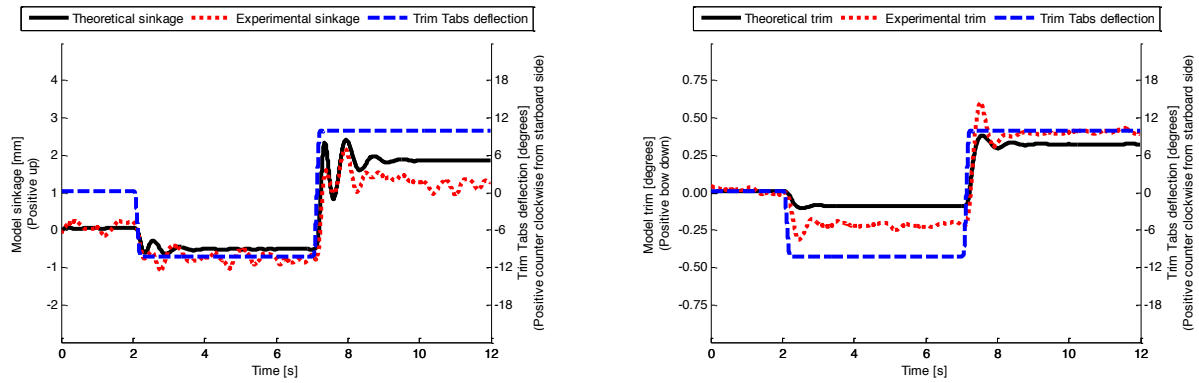


Figure 13: Model responses to stern tabs deflection of $\pm 10^\circ$ at model speed of 2.89m/s

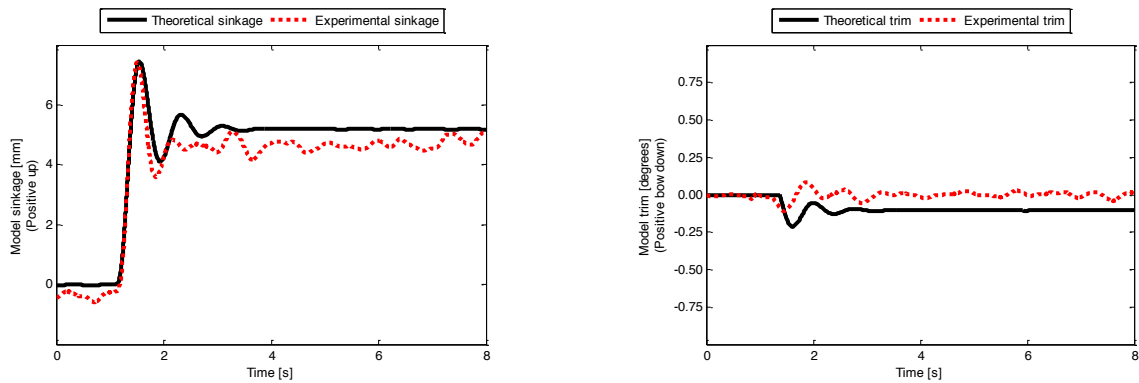


Figure 14: Model responses to step movements of RCS surfaces when activated together (T-Foil deflection of $+15^\circ$ and stern tabs deflection of $+10^\circ$) to produce only a sinkage change at model speed of 2.89m/s

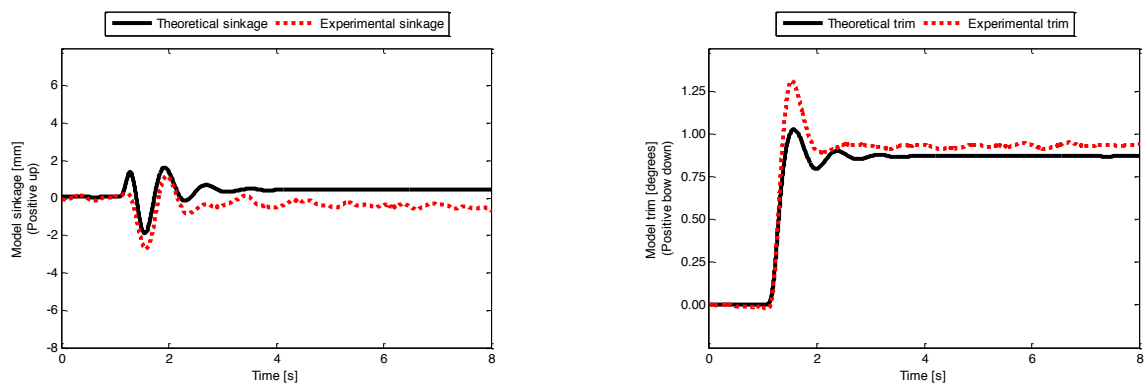


Figure 15: Model responses to step movements of RCS surfaces when activated together (T-Foil deflection of -8° and stern tabs deflection of $+18^\circ$) to produce only a trim change at model speed of 2.89m/s